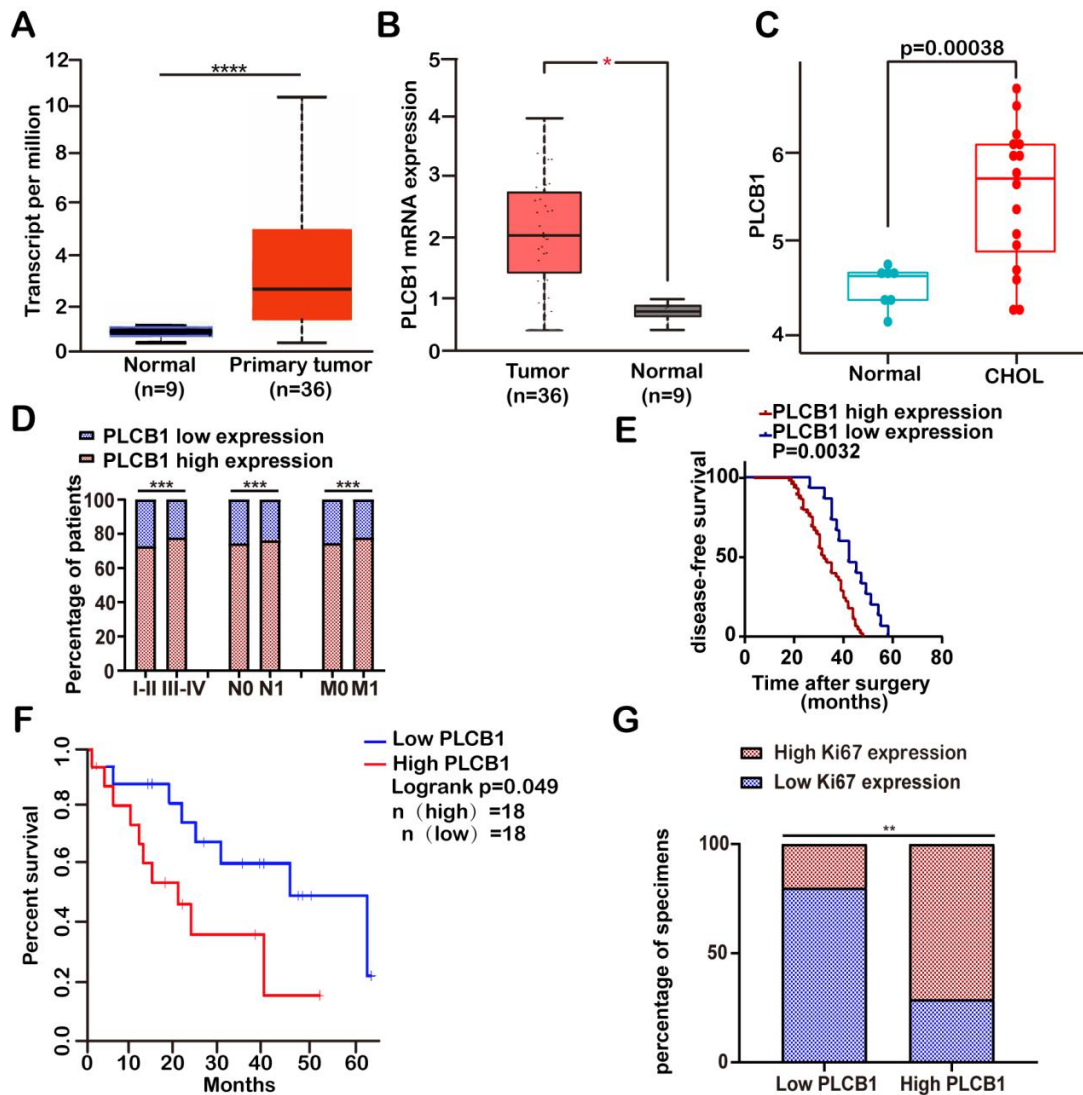


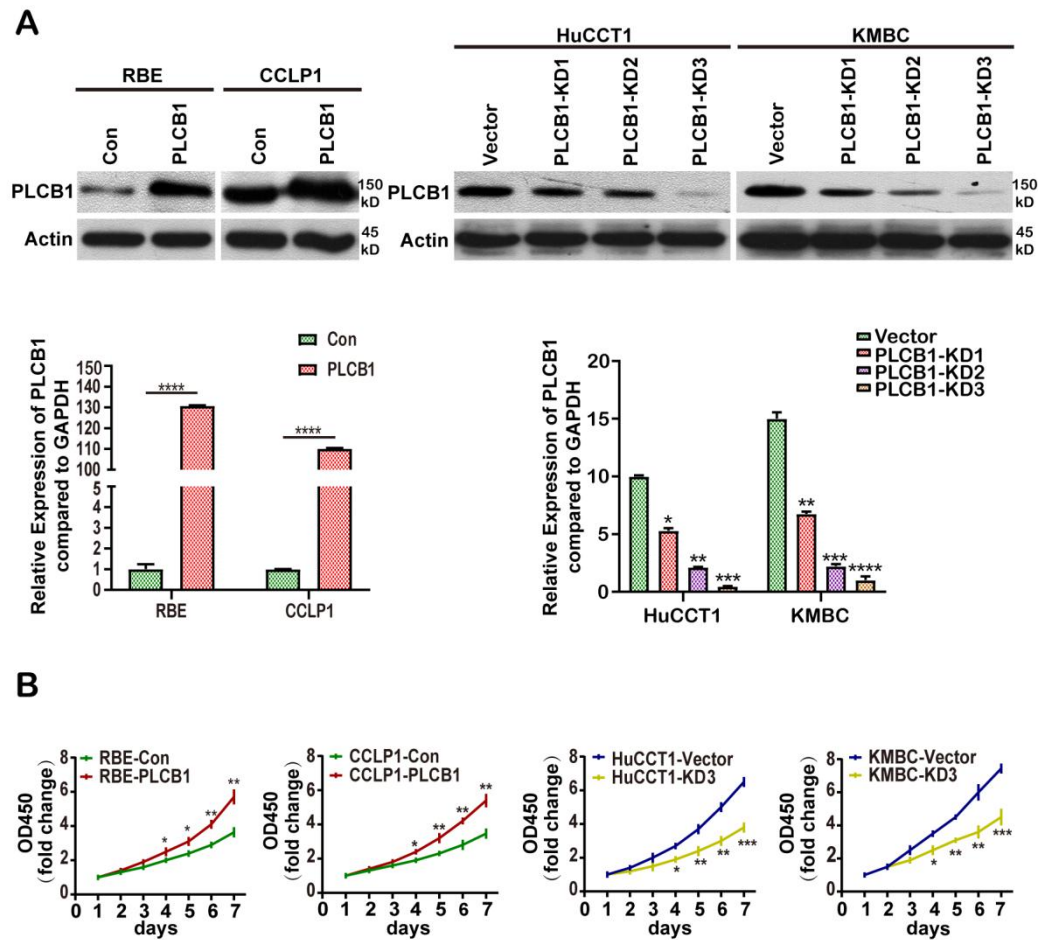
### Supplement Figure 1

**Fig.S1. Screening of genes to be studied.** (A) Volcano plot of differential expression genes from the TCGA CHOL data.  $|\log_2 \text{ Fold Change}| > 1$  & adjusted P value  $< 0.05$  were considered as significant (CHOL vs. Normal). (B) Venn diagram of three gene sets.



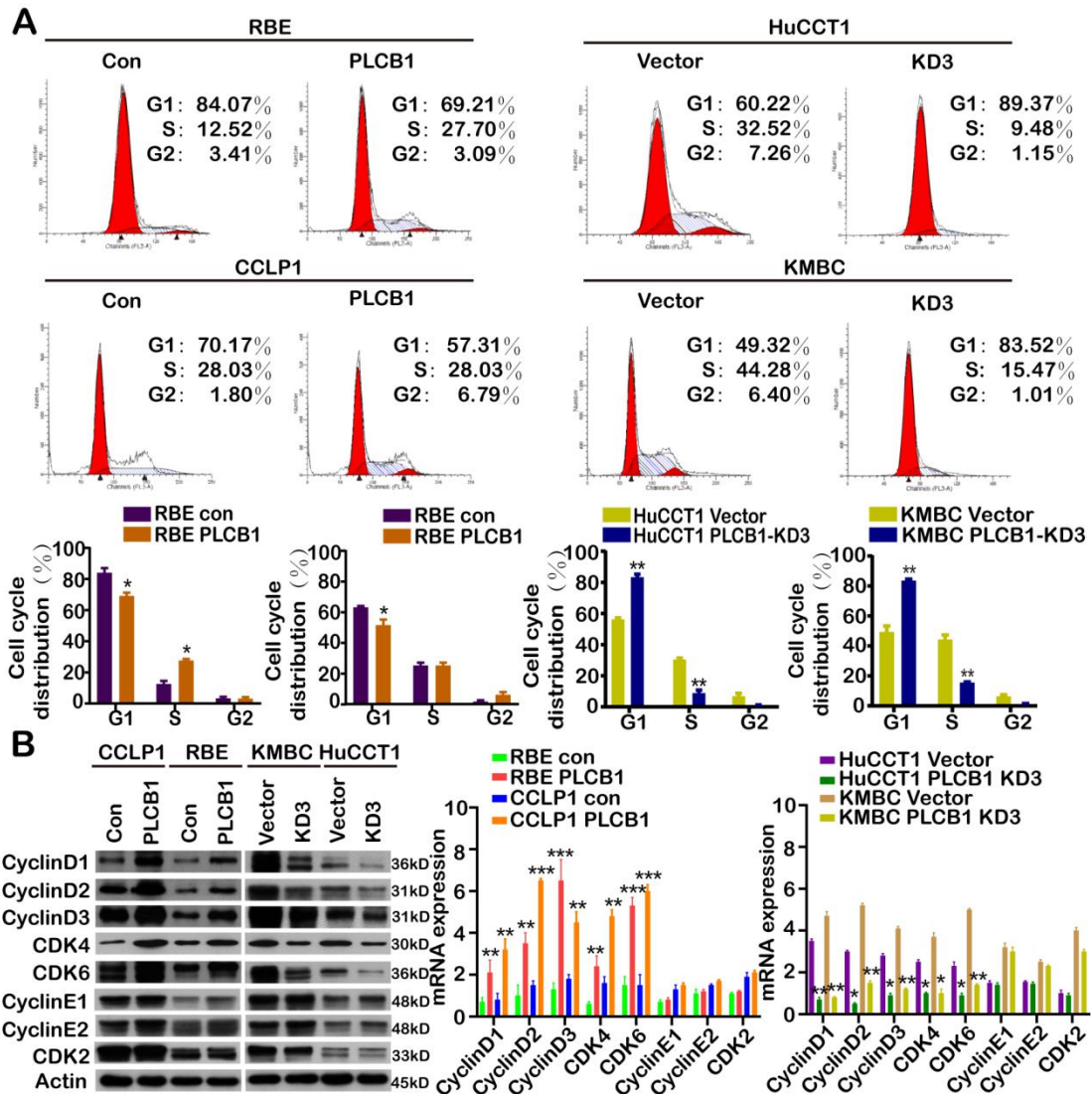
## Supplement Figure 2

**Fig.S2. Clinical characteristics of PLCB1.** (A-B) The TCGA data from the ULCAN and GEPIA database website indicated that PLCB1 expression was strikingly higher in human CCA tissues than that in the tissues adjacent to cancer. (C) GEO database (GSE32879) demonstrated that PLCB1 expression was higher in human CCA tissues compared to adjacent tissues. CHOL: human CCA tissues. (D) Percentage of patients with upregulated and downregulated PLCB1 according to the cancer staging, lymph node status and metastasis. I-II: TNM I-II stage. III-IV: TNM III-IV stage. N0: no lymph node metastasis. N1: lymph node metastasis. M0: no distant metastasis. M1: distant metastasis. \*\*\*  $p < 0.001$ , based on the one-way ANOVA. (E) The influence of strong or weak PLCB1 staining on DFS was analyzed by Kaplan-Meier plot. DFS: disease-free survival. (F) The TCGA data from the GEPIA database website showed that upregulated PLCB1 heralded a shorter lifespan. (G) 32 of 45 CCA human tissues with high PLCB1 expression exhibited a high level of Ki-67, whereas 12 of 15 CCA human tissues with low PLCB1 expression showed a low level of Ki-67, suggesting that PLCB1 expression was closely correlated with CCA proliferation. \*\* $p < 0.01$ , based on Student's t test.



### Supplement Figure 3

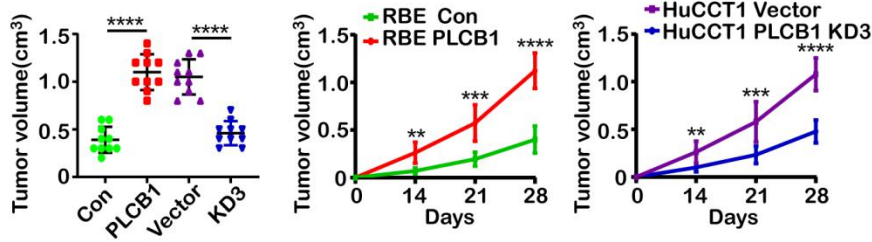
**Fig.S3. Confirmation of PLCB1 knockout or overexpression in CCA cell lines.** (A) Western blot and qRT-PCR verified PLCB1 overexpression and knockdown efficiency for indicated CCA cell lines. Con: PLCB1 overexpression negative control. PLCB1: PLCB1 overexpression. Vector: PLCB1 knockdown negative control. PLCB1-KD1-3: PLCB1 knockdown. \*\*\*\* $p < 0.0001$ , based on Student's t test. (B) Growth curves were analyzed by CCK-8 assays. \* $p < 0.05$ ; \*\* $p < 0.01$ ; \*\*\* $p < 0.001$ , based on Student's t test. All experiments were implemented three times and data are presented as mean  $\pm$  SD.



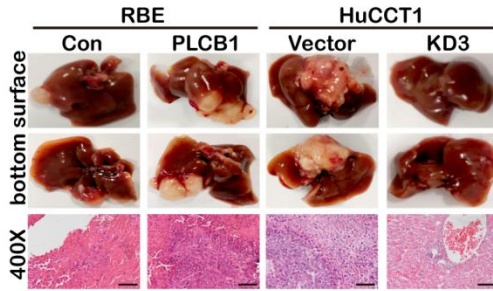
**Supplement Figure 4**

**Fig.S4. Ectopic PLCB1 enhances G1/S transition of indicated CCA cell lines.** (A) Cell cycle analysis predicted the G1 to S phase for indicated CCA cell lines was affected by overexpression and knockdown PLCB1. \* $p < 0.05$ ; \*\* $p < 0.01$ , based on Student's t test. (B) Western blot and qRT-PCR demonstrated that overexpression and knockdown PLCB1 had impact on key proteins controlling G1/S transition, such as cyclinD1, cyclinD2, cyclinD3, CDK4 and CDK6. \* $p < 0.05$ ; \*\* $p < 0.01$ ; \*\*\* $p < 0.001$ , based on Student's t test. All experiments were implemented three times and data are presented as mean  $\pm$  SD.

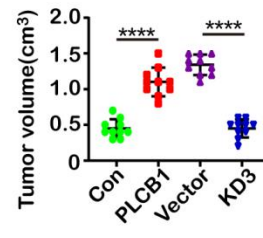
**A**



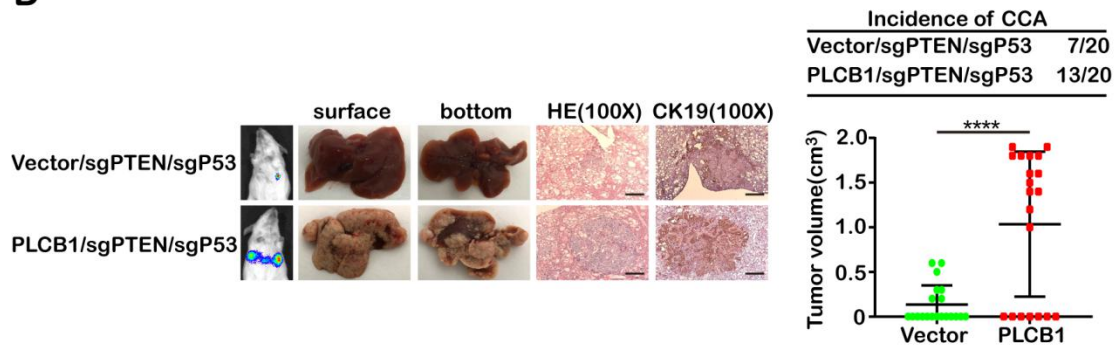
**B**



**C**

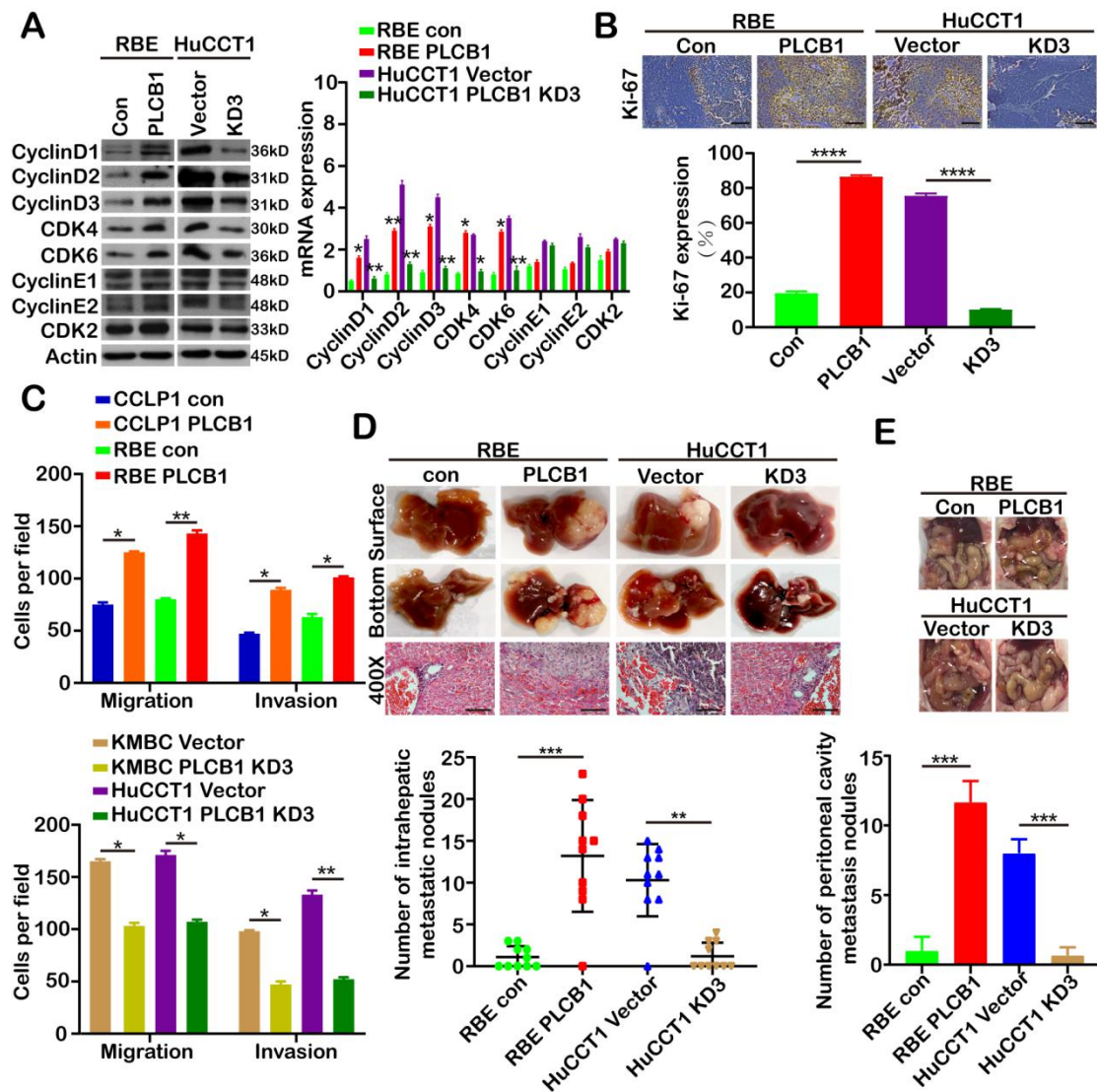


**D**



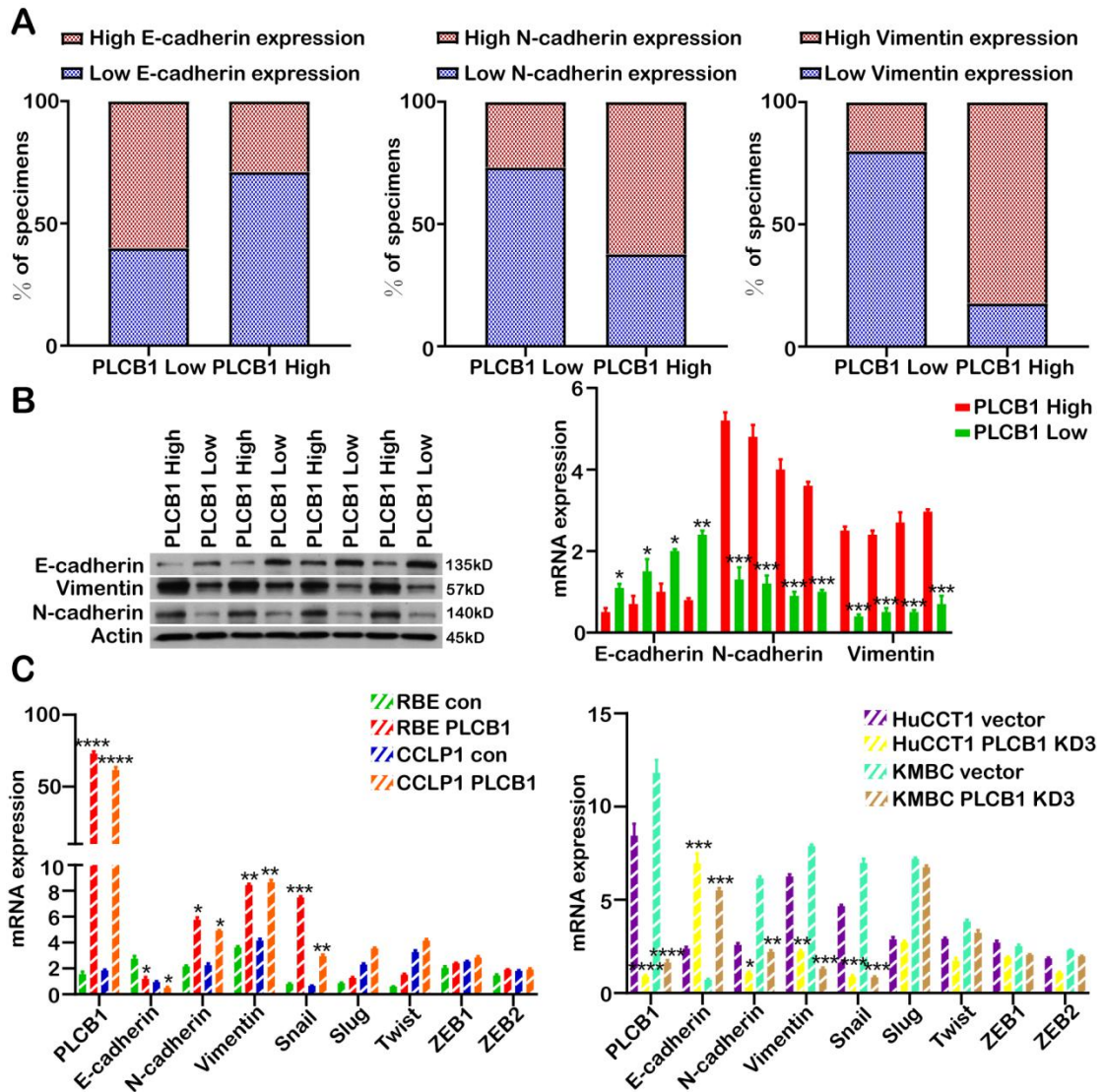
**Supplement Figure 5**

**Fig.S5. Ectopic PLCB1 promotes CCA tumorigenesis and proliferation *in vivo*.** (A) Subcutaneous xenograft tumor volumes were measured for indicated groups. \*\*\*\* $p < 0.0001$ , based on Student's t test. (B) Typical images of orthotopic xenograft mice models and H&E staining. Scale bars: 400X= 100 $\mu$ m. (C) Orthotopic xenograft tumor volumes were measured for indicated groups. \*\*\*\* $p < 0.0001$ , based on Student's t test. (D) Typical images of bioluminescence pictures, H&E and CK19 staining of vector/sgPTEN/sgP53 and PLCB1/sgPTEN/sgP53 female FVB/N (H2d) mouse livers at 8 weeks after hydrodynamic injection respectively. \*\*\*\*  $p < 0.0001$ , based on Student's t test. Scale bars: 100X= 400 $\mu$ m. All experiments were implemented three times and data are presented as mean  $\pm$  SD.



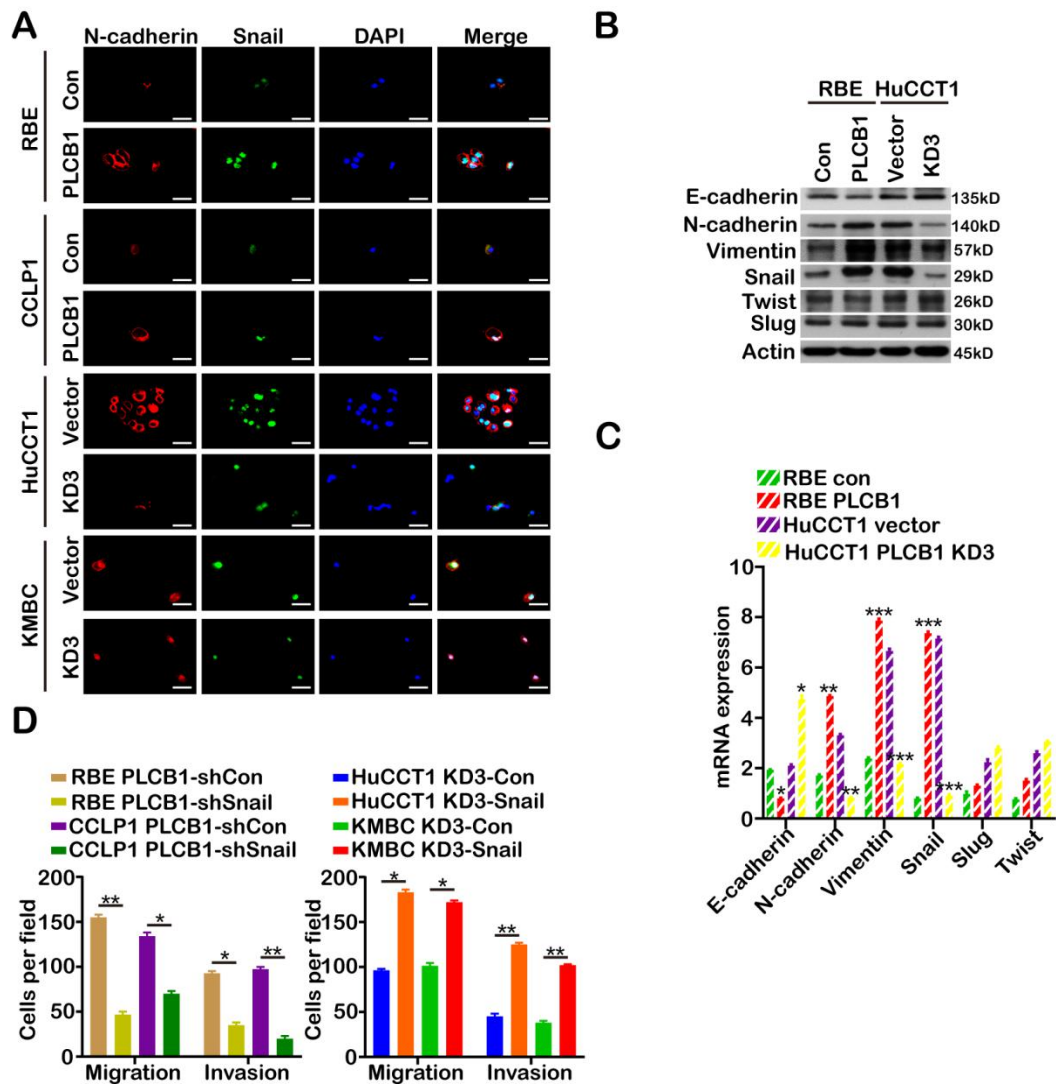
**Supplement Figure 6**

**Fig.S6. PLCB1 promotes CCA migration and metastasis.** (A) Western blot and qRT-PCR showed that the G1/S transition key proteins of subcutaneous tumor tissues in PLCB1 overexpression groups presented high levels, whereas knockdown PLCB1 groups had reverse results.  $*p < 0.05$ ;  $**p < 0.01$ , based on Student's t test. (B) Typical IHC images of the relationship between Ki-67 expression and subcutaneous tumors in the RBE- PLCB1 group and the HuCCT1-PLCB1-KD3 group.  $****p < 0.0001$ , based on Student's t test. Scale bars: 400X=100 $\mu$ m. (C) Number of cells in migration and invasion assays for indicated CCA cell lines.  $*p < 0.05$ ;  $**p < 0.01$ , based on Student's t test. (D) Typical images of mice liver metastasis and H&E staining of liver metastasis and number of metastatic nodules.  $**p < 0.01$ ;  $***p < 0.001$ , based on Student's t test. Scale bars: 400X=100 $\mu$ m. (E) Typical images of mice peritoneal cavity metastasis and number of metastatic nodules.  $***p < 0.001$ , based on Student's t test. All experiments were implemented three times and data are presented as mean  $\pm$  SD.



**Supplement Figure 7**

**Fig.S7. The relationship between EMT related markers and CCA samples.** (A) The expression of PLCB1 was associated with the EMT related markers. (B) Western blot and qRT-PCR analyzed the relationship between PLCB1 and the EMT related markers in human CCA tissues. \* $p < 0.05$ ; \*\* $p < 0.01$ ; \*\*\* $p < 0.001$ , based on Student's t test. (C) qRT-PCR demonstrated that PLCB1 overexpression and knockdown affected the levels of the EMT related markers and snail. \* $p < 0.05$ ; \*\* $p < 0.01$ ; \*\*\* $p < 0.001$ , based on Student's t test. All experiments were implemented three times and data are presented as mean  $\pm$  SD.



Supplement Figure 8

**Fig.S8. Snail is closely associated with the EMT process induced by PLCB1.** (A) Typical IF images of the expression of N-cadherin and snail for indicated CCA cell lines. Scale bars: 400X=100 $\mu$ m. (B) The protein expression of the EMT related markers and snail in mouse tumor-forming tissues was evaluated by western blot. (C) The mRNA expression of the EMT related markers and snail in mouse tumor-forming tissues was evaluated by qRT-PCR. \* $p$ <0.05; \*\* $p$ <0.01; \*\*\* $p$ <0.001, based on Student's t test. (D) Histograms of migration and invasion assays demonstrated that upregulated and downregulated snail restored the number of the RBE-PLCB1 group and the HuCCT1-PLCB1-KD3 group. \* $p$ <0.05; \*\* $p$ <0.01, based on Student's t test. All experiments were implemented three times and data are presented as mean  $\pm$  SD.

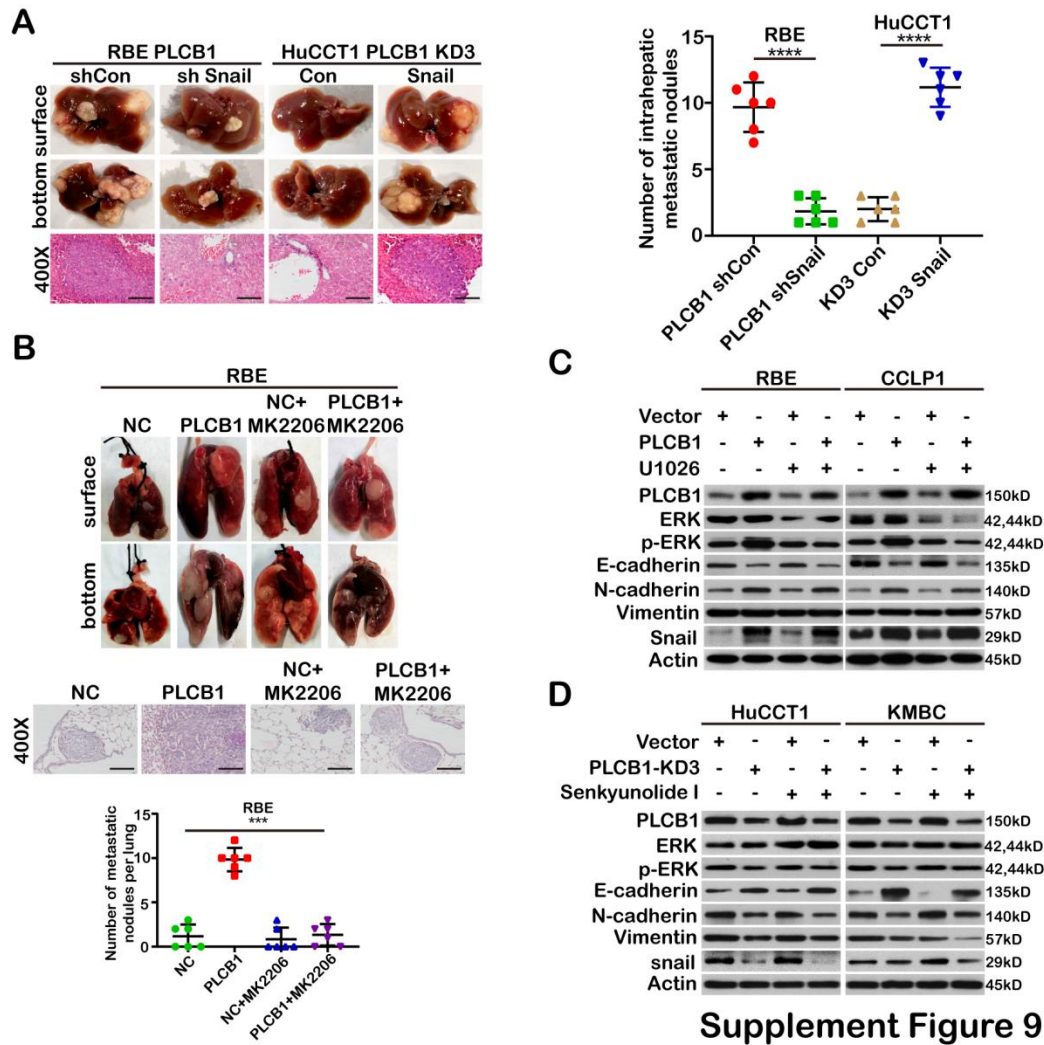
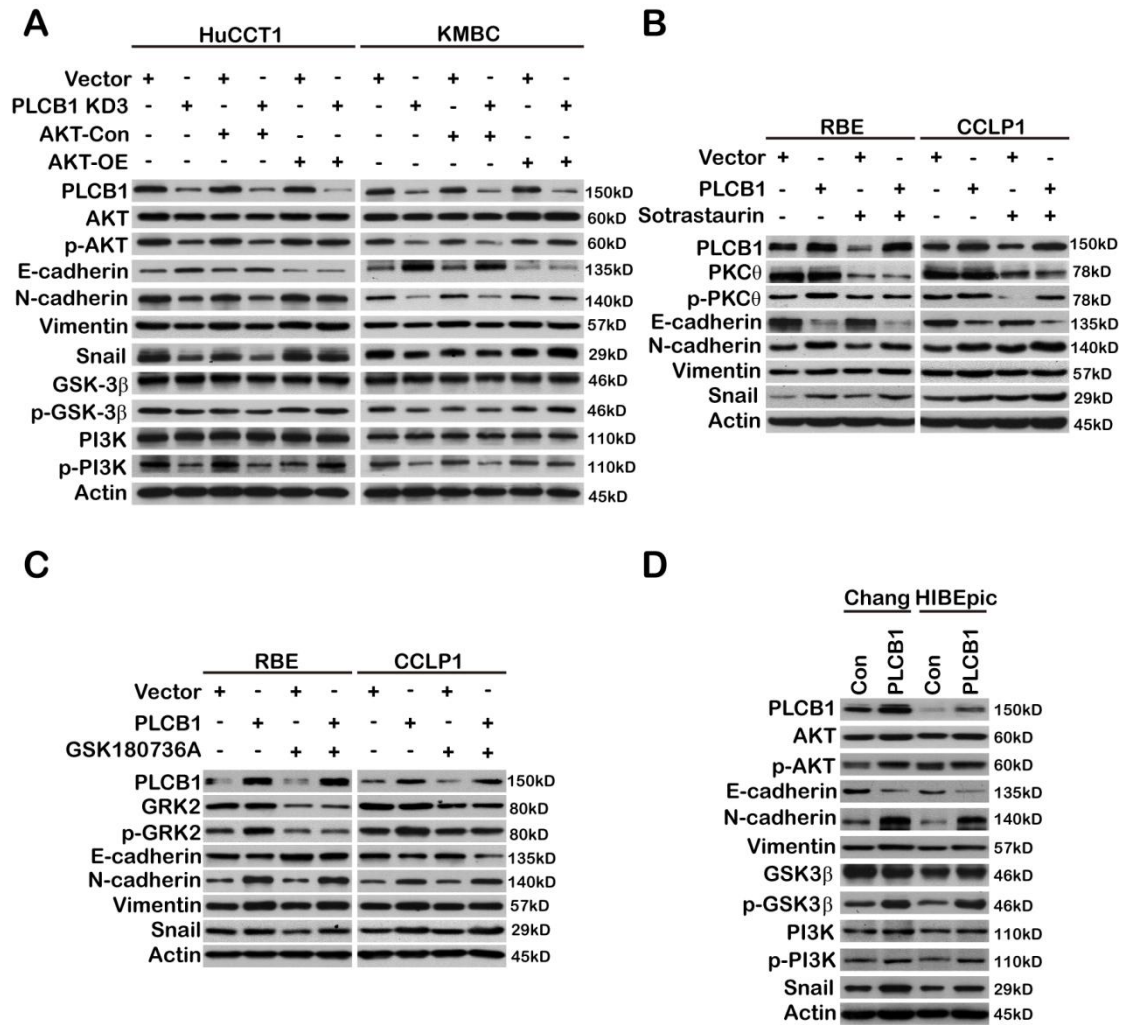
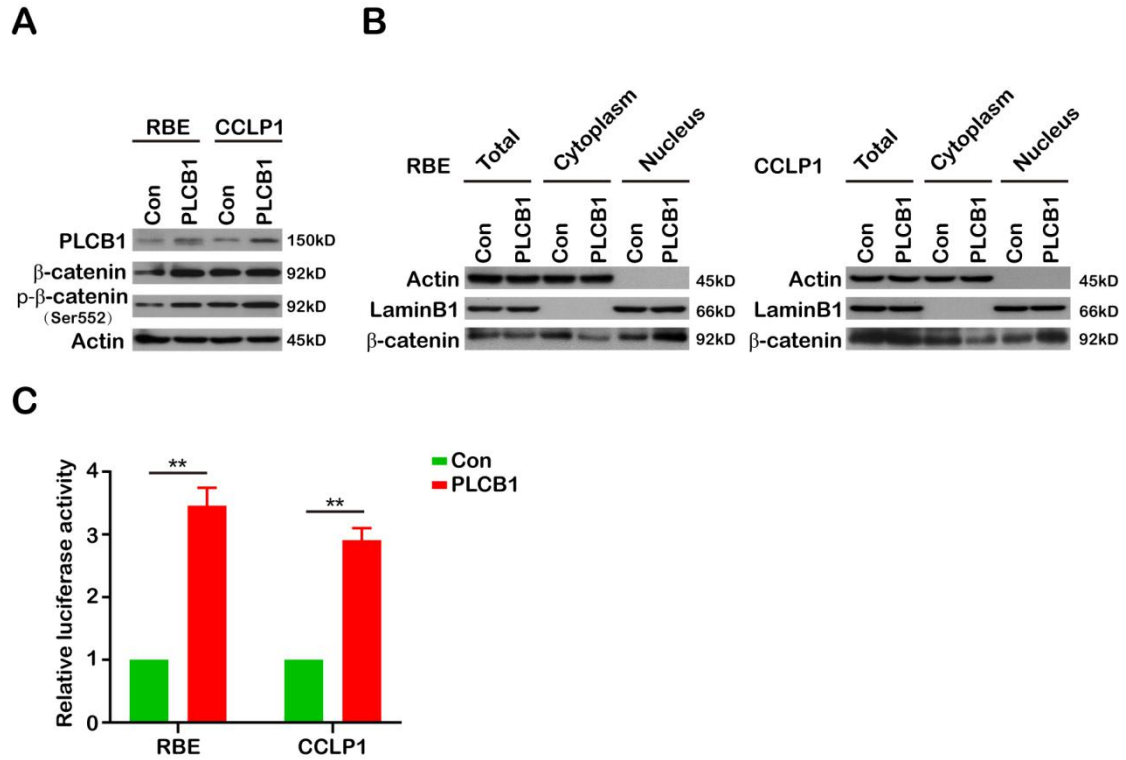


**Fig.S9. PLCB1 induces EMT process via PI3K/AKT/GSK3 $\beta$ /snail signaling pathway.** (A) Typical images of liver metastasis and H&E staining for indicated CCA cell lines which snail was overexpressed and knocked down. \*\*\*\* $p < 0.0001$ , based on Student's t test. Scale bars: 400X=100 $\mu$ m. (B) Typical images of mice lung metastasis which administered with MK2206 (60mg/kg) three weeks and H&E staining. NC: negative control. PCB1: PCB1 overexpression. NC+MK2206: negative control plus MK2206. PCB1+MK2206: PCB1 overexpression plus MK2206. \*\*\* $p < 0.001$ , based on Student's t test. Scale bars: 400X=100 $\mu$ m. (C) The expression levels of the EMT related markers, snail, ERK and p-ERK were analyzed by western blot after the treatment of 40 $\mu$ mol U1026. (D) The expression levels of EMT related markers, snail, ERK and p-ERK were analyzed by western blot after the treatment of 50 $\mu$ mol senkyunolide I. All experiments were implemented three times and data are presented as mean  $\pm$  SD.



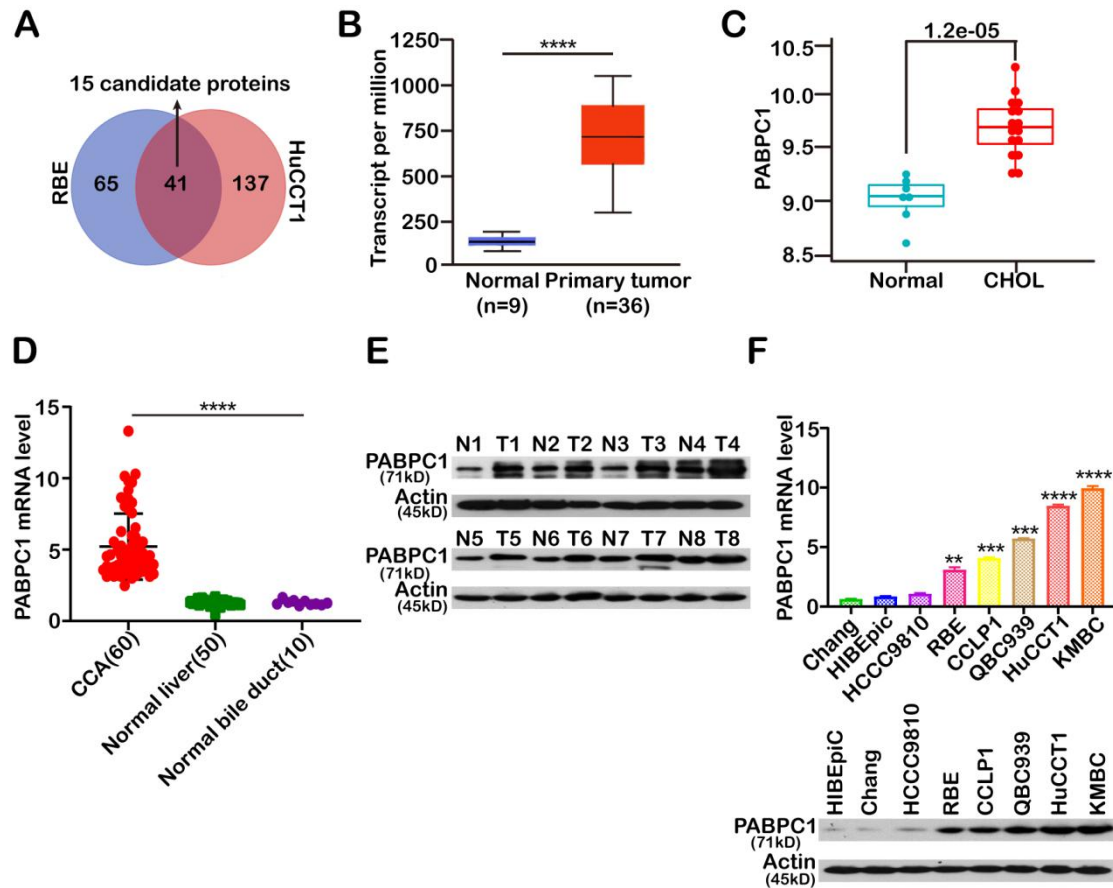
### Supplement Figure 10

**Fig.S10. AKT pathway is vital for PLCB1 to induce EMT.** (A) The expression levels of key proteins of the EMT process and PI3K/AKT pathway were evaluated by western blot after transfection with lentivirus AKT-con and AKT overexpression for indicated CCA cell lines. AKT-con: AKT overexpression negative control. AKT-OE: AKT overexpression. (B) The expression levels of the EMT related markers, snail, PKC $\theta$  and p- PKC $\theta$  were analyzed by western blot after the treatment of 4 $\mu$ mol sotrastaurin. (C) The expression levels of the EMT related markers, snail, GRK2 and p-GRK2 were analyzed by western blot after the treatment of 0.8 $\mu$ mol GSK180736A. (D) The expression levels of key proteins of the EMT process and PI3K/AKT pathway were evaluated by western blot in overexpressed PLCB1 normal bile duct and liver cell lines. All experiments were implemented three times and data are presented as mean  $\pm$  SD.



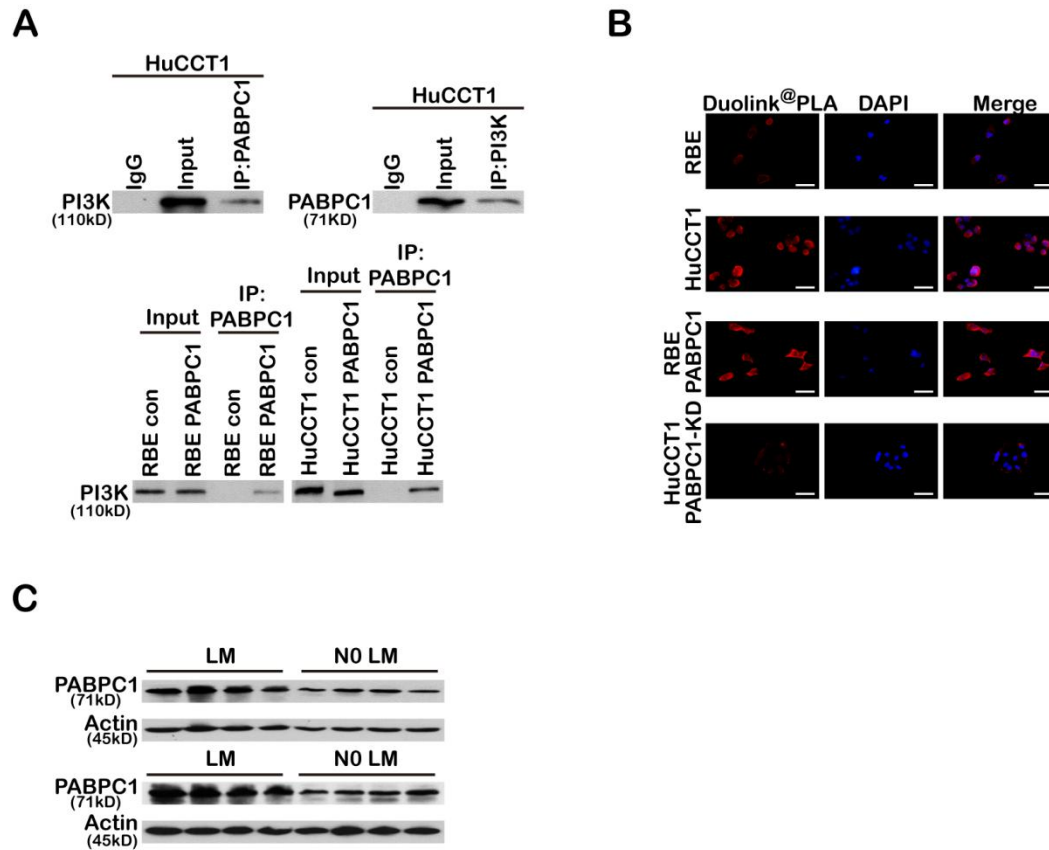
### Supplement Figure 11

**Fig.S11. Overexpressing PLCB1 enhanced the levels of  $\beta$ -catenin and phospho  $\beta$ -catenin and nuclear accumulation.** (A) Western blot analysis of  $\beta$ -catenin and phospho  $\beta$ -catenin for indicated cell lines. (B) Western blot analysis of total, cytosol and nuclear fractions derived from RBE-Con, RBE-PLCB1, CCLP1-Con and CCLP1-PLCB1 cell lines. (C) RBE-Con, RBE-PLCB1, CCLP1-Con and CCLP1-PLCB1 cell lines were co-transfected with renilla luciferase and REPO<sup>TM</sup>TCF/LEF1 luciferase reporter plasmids. Luciferase activity was determined after 24h. \*\* $p < 0.01$ , based on Student's t test. All experiments were implemented three times and data are presented as mean  $\pm$  SD.



### Supplement Figure 12

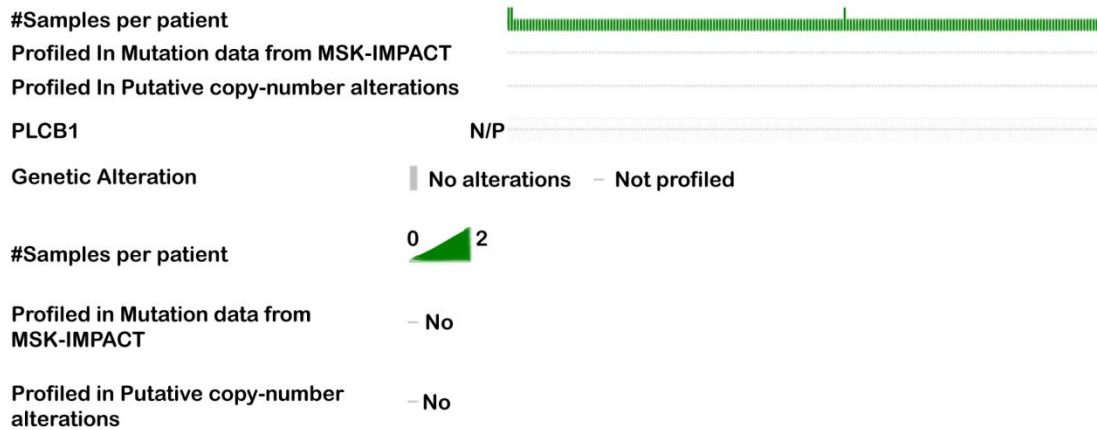
**Fig.S12. PABPC1 is highly expressed in CCA tissues and is closely associated with metastasis.** (A) Schematic diagram of mass spectrometry. (B) The TCGA data from the ULCAN database website revealed that PABPC1 expression was strikingly higher in human CCA tissues than that in tissues adjacent to cancer. (C) Data from GEO database (GSE32879) demonstrated that PABPC1 was upregulated in human CCA tissues compared to adjacent tissues. CHOL: CCA tissues. (D-E) qRT-PCR and western blot indicated that PABPC1 mRNA and protein levels in 60 human CCA tissues compared to adjacent tissues (10 normal bile duct and 50 normal liver ). T: tumors; N: adjacent normal tissues. \*\*\*\* $p < 0.0001$ , based on Student's t test. (F) PABPC1 mRNA and protein levels in CCA cell lines compared to normal liver (Chang) and normal human intrahepatic biliary (HIBEpic) cell lines were evaluated by qRT-PCR and western blot. \*\* $p < 0.01$ ; \*\*\* $p < 0.001$ ; \*\*\*\* $p < 0.0001$ , based on the one-way ANOVA. All experiments were implemented three times and data are presented as mean  $\pm$  SD.



### Supplement Figure 13

**Fig.S13. PABPC1 interacts with PI3K.** (A) Endogenous and exogenous coimmunoprecipitation (co-IP) indicated that PABPC1 could interact with PI3K. (B) Typical images of the Duolink<sup>®</sup> PLA experiment predicted PABPC1 directly interacted with PI3K via the fluorescence microscope. Scale bars: 400X=100 $\mu$ m. (C) Typical images of PABPC1 protein levels in CCA patients with or without lymph node metastasis. LM: lymph node metastasis; NO LM: no lymph node metastasis. All experiments were implemented three times and data are presented as mean  $\pm$  SD.

**A**

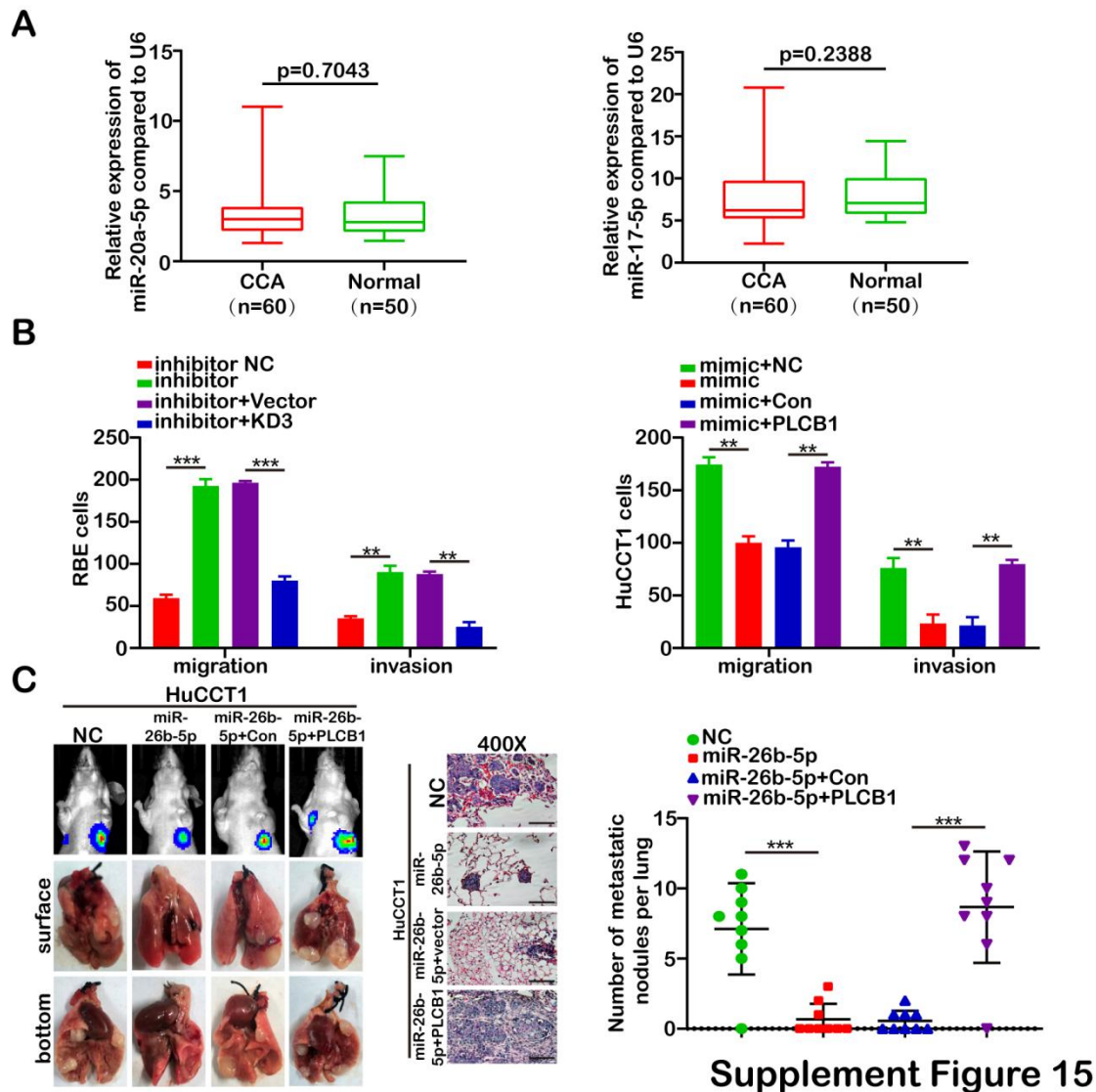


**B**



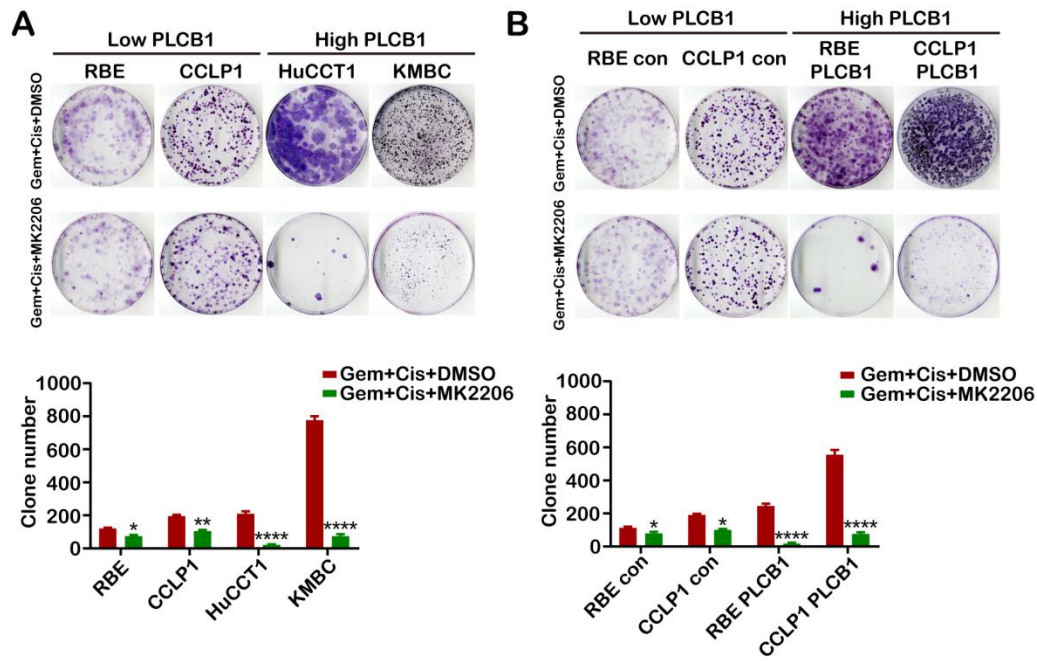
## Supplement Figure 14

**Fig.S14. Two public data on cholangiocarcinoma from the cBioPortal database.** (A-B) The cBioPortal for Cancer Genomics is an open-access, open-source resource for interactive exploration of multidimensional cancer genomics data sets. Genetic data types integrated in cBioPortal include somatic mutations, DNA copy number alterations, mRNA and microRNA expression, DNA methylation, protein abundance, and phosphoprotein abundance. Two public data on cholangiocarcinoma with a sample size of more than 100 cases, including MSK-IMPACT study (n =195) and Shanghai study (n =103), were retrieved from the cBioPortal database. In the "Query By Gene" module, we entered "PLCB1" to view its mutation and DNA copy number variation in cholangiocarcinoma.



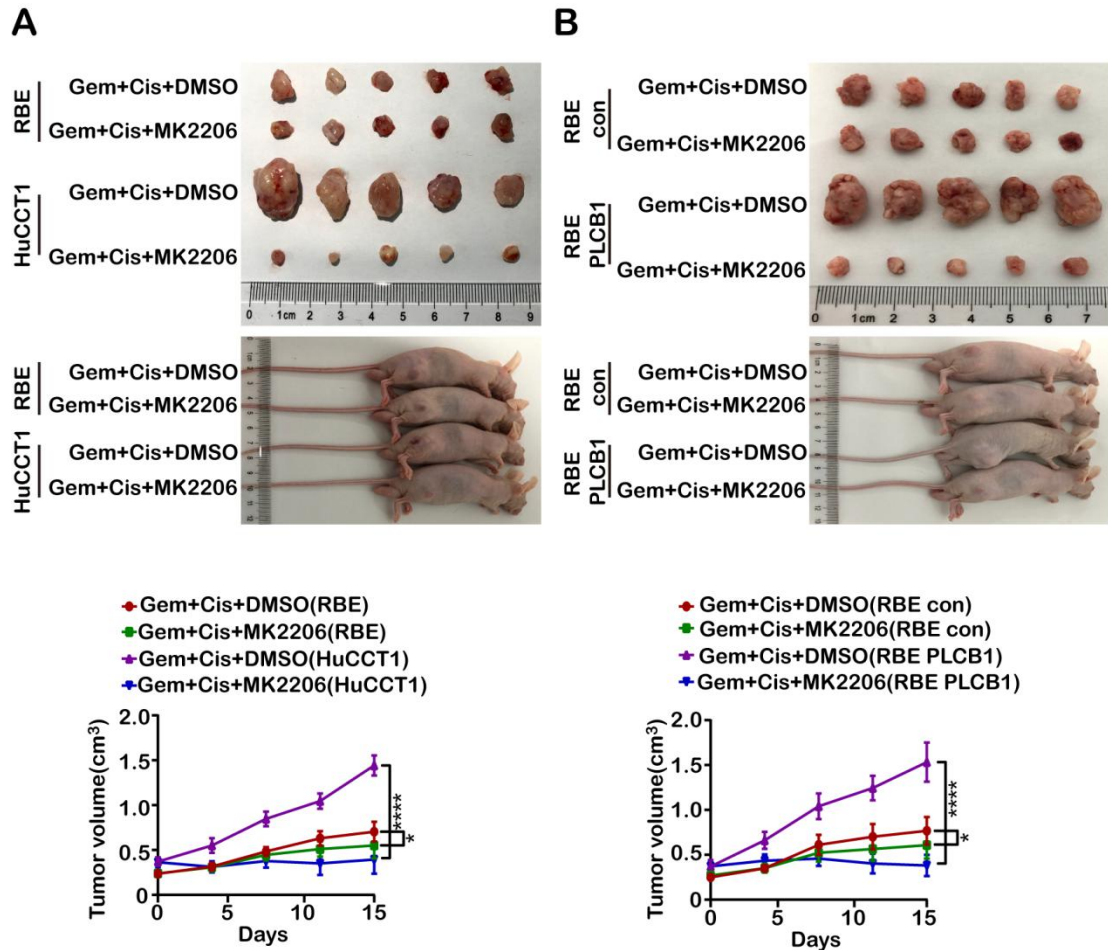
Supplement Figure 15

**Fig.S15. MiR-26b-5p suppresses CCA metastasis which PLCB1 participated in.** (A) MiR-20a-5p and miR-17-5p expression levels in human CCA tissues compared to adjacent tissues were analyzed by qRT-PCR. Based on Student's t test. (B) Migration and invasion assays proved that miR-26b-5p mimics and inhibitor could restore the cell numbers of the RBE-PLCB1 group and the HuCCT1-PLCB1-KD3 group.  $**p<0.01$ ;  $***p<0.001$ , based on Student's t test. (C) Typical images of mice lung metastasis and H&E staining for indicated groups. NC: miR-26b-5p mimic negative control. miR-26b-5p: miR-26b-5p mimic. miR-26b-5p+Con: miR-26b-5p mimic plus PLCB1 overexpression negative control. miR-26b-5p+PLCB1: miR-26b-5p mimic plus PLCB1 overexpression.  $***p<0.001$ , based on Student's t test. Scale bars: 400X=100 $\mu$ m. All experiments were implemented three times and data are presented as mean  $\pm$  SD.



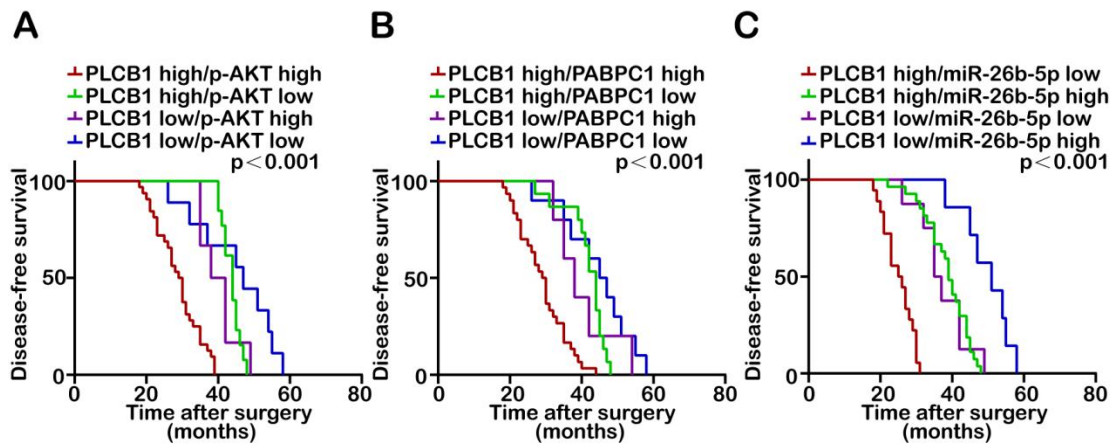
Supplement Figure 16

**Fig.S16. MK2206 can restrain the chemotherapy resistance of gemcitabine combined with cisplatin induced by ectopic PLCB1.** (A-B) Colony formation was quantified by crystal violet staining after 14 days of treatment with gemcitabine (Gem,1 $\mu$ M) plus cisplatin (Cis,10 $\mu$ M) or gemcitabine, cisplatin plus MK2206 (0.2 $\mu$ M). \* $p$ <0.1; \*\* $p$ <0.01; \*\*\*\* $p$ <0.0001, based on Student's t test. All experiments were implemented three times and data are presented as mean  $\pm$  SD.



Supplement Figure 17

**Fig.S17. Establishing an *in vivo* therapeutic mouse model to detect MK2206 can inhibit the chemotherapy resistance of gemcitabine combined with cisplatin induced by ectopic PLCB1.** (A-B) Differences between gross findings at the end of the 15-day experimental period and average tumor volumes on different experimental days in mice treated with gemcitabine (Gem, 200 mg/kg) plus cisplatin (Cis, 5 mg/kg) or gemcitabine, cisplatin plus MK2206 (60mg/kg). \* $p < 0.1$ ; \*\* $p < 0.01$ ; \*\*\*\* $p < 0.0001$ , based on Student's t test. All experiments were implemented three times and data are presented as mean  $\pm$  SD.



### Supplement Figure 18

**Fig.S18. Taking advantage of a combination of two parameters increases the prognostic value, compared to using PLCB1 alone.** (A) Kaplan–Meier analysis of disease-free survival in patients with variable expressions of PLCB1 and p-AKT. (B) Kaplan–Meier analysis of disease-free survival in patients with variable expressions of PLCB1 and PABPC1. (C) Kaplan–Meier analysis of disease-free survival in patients with variable expressions of PLCB1 and miR-26b-5p.